

# Magnetic resonance microimaging indicates water diffusion correlates with dormancy induction in cultured hybrid poplar (*Populus* spp.) buds

LEE KALCSITS,<sup>1,2</sup> EDWARD KENDALL,<sup>3,4</sup> SALIM SILIM<sup>1</sup> and KAREN TANINO<sup>2</sup>

<sup>1</sup> PFRA Shelterbelt Centre, Agriculture and Agri-Food Canada, Indian Head, SK, Canada

<sup>2</sup> Department of Plant Sciences, College of Agriculture and Bioresources, University of Saskatchewan, Saskatoon, SK, Canada

<sup>3</sup> Discipline of Radiology, Faculty of Medicine, Janeway Child Health Centre, Memorial University of Newfoundland, St. John's, NL, A1B 3V6, Canada

<sup>4</sup> Corresponding author (Edward.kendall@mun.ca)

Received May 21, 2009; accepted July 3, 2009; published online August 20, 2009

**Summary** Water content and mobility, which are factors known to be associated with dormancy induction in woody plants on a tissue level, were measured using non-destructive magnetic resonance microimaging (MRMI). Two cultured poplar clones ('Okane' – temperature-insensitive dormancy and 'Walker' – temperature-sensitive dormancy) were subjected to dormancy differentiating temperature regimes, 18.5/3.5 °C and 18.5/13.5 °C (day/night), under a short photoperiod. Apparent diffusion coefficient, an indicator of water mobility, correlated with dormancy development in the axillary bud and vascular bud trace regions. In contrast,  $T_1$  relaxation time, an indicator of static biophysical water properties, did not correlate significantly with dormancy in the regions that were examined. Although MRMI studies using  $T_1$  relaxation measurements have dominated the phytological field, our work indicates that water mobility is an important factor in studies examining water changes during dormancy induction in the critical tissues of woody plants.

**Keywords:**  $T_1$  relaxation.

## Introduction

The connection between dormancy and water status has been extensively studied (Faust et al. 1991, 1995, Li et al. 2003); nevertheless, localized changes within a plant tissue have been difficult to elucidate. During dormancy induction, the water content of plant tissue decreases (Rinne et al. 1994, Jeknic and Chen 1999), particularly in the axillary bud (Li et al. 2003). Where dormancy is photoperiod sensitive, short photoperiods cause growth cessation and reduced water content. These are observed as tandem processes, but the details of any linkage are not perfectly understood.

Water is the essential medium for many metabolic processes; moderating its availability impacts metabolic activity and, in turn, growth. Biological water-modulation strategies include bulk transport from the plant to the environment or to non-critical areas in the plant. At the cellular level, water activity is modulated by hydrophilic molecules, such as sugars and dehydrin proteins. These compounds accumulate during dormancy induction and cold acclimation and change both the osmotic potential of water and its availability (Kuroda and Sagisaka 2001). Regional macroscopic events such as osmotic balance, membrane permeability and aquaporin distribution may also impact the movement of water between cellular and extracellular spaces (Yooyongwech et al. 2008). These considerations suggest that understanding the physical state, the chemical potential and the relative mobility of water will enhance our understanding of dormancy development and its regulation in cultured poplar buds.

Whole plant methods for evaluating water content are often destructive and do not provide information on the state and distribution of residual water fractions. Nuclear magnetic resonance (NMR)-based measurements are an attractive, non-destructive alternative. It allows measurement of a variety of biophysical parameters, including diffusion, viscosity and solute status. Measurements can be made by averaging over the whole organism or by selecting the regions of interest (ROI) using non-invasive imaging protocols. For spectroscopic studies, a variety of magnetically active nuclei are available; for imaging studies,  $^1\text{H}$  (the hydrogen nucleus) offers the greatest sensitivity (Morris 1986; cited in Connelly et al. 1987). Spectroscopic and imaging protocols can be combined so that high-resolution (a typical spatial resolution is 50  $\mu\text{m} \times 50 \mu\text{m}$ ), non-destructive measurements of biophysical interactions occurring within the plant tissue (Ishida 2000) are possible using magnetic resonance microimaging (MRMI). MRMI-based dormancy studies include seed

germination (Connelly et al. 1987, Hou et al. 1997) and bud dormancy (Faust et al. 1991, Erez et al. 1998, Fennell and Line 2001, Yooyongwech et al. 2008). It is interesting to note that earlier attempts to relate water status to dormancy in woody species axillary buds and vascular tissue were inconclusive (Faust et al. 1991).

The NMR measurements require that the nucleus of interest (in this case, the water proton,  $^1\text{H}$ ) be excited by a brief pulse of energy. Relaxation measurements reflect the rate at which the signal from the excited nuclei disappears. There are two processes involved: one that results in the added energy being transferred to the environment (characterized by the time constant  $T_1$ ) and those processes that disperse the signal from the excited cohort (characterized by the time constant  $T_2$ ). The ability to weight images based on  $T_1$  or  $T_2$  (or to calculated time constant maps) has led to the notion of considering these as 'stains' reflecting the biophysical properties (including viscosity and solute concentration) of the tissue water (Belton and Ratcliffe 1985; cited in Snaar and Van As 1992).

Investigations of water changes during dormancy have used NMR imaging during dormancy induction, maintenance and release (Faust et al. 1991, Gardea et al. 1994, Fennell et al. 1996, Erez et al. 1998, De Fay et al. 2000). Several of these studies measured  $T_1$  and/or  $T_2$  relaxation times (Faust et al. 1991, 1995, Fennell et al. 1996, Gardea et al. 1994, Erez et al. 1998). Although these parameters may reflect changes in local water content and binding within the plant tissue, the  $T_1$  and/or  $T_2$  relaxation times do not provide any insight into water translational mobility. Identifying changes in water mobility is paramount for completely elucidating water changes during dormancy because cell-to-cell communication including the movement of water and metabolites is necessary for growth-related metabolic activity (Yooyongwech et al. 2008).

Water mobility within the plant tissue can be measured using MRMI by producing images weighted for diffusion (or flow) where the contrast is derived from average mobility within the volume element. Often, multiple diffusion measurements are taken over a range of diffusivities, allowing the calculation of an apparent diffusion coefficient (ADC) for every volume element (Tanner 1983). This diffusion map forms the basis of subsequent calculations. For example, Hou et al. (1997) used diffusion-weighted imaging to determine localized water uptake in *Avena fatua* L. seeds during germination. Diffusion-weighted imaging has been used sparingly to study tissue dormancy. De Fay et al. (2000) used diffusion-weighted images to show increases in water movement and activity during budburst in *Picea abies* (L.) Karst. buds after fulfillment of its chilling requirement. Diffusion-weighted images were used to assess water mobility (proportional to ADC value) in *Tulipa* spp. bulbs during chilling (Van der Toorn et al. 2000). Past investigations had been limited by technical constraints such as low magnetic field strength and large field of view, which are factors that limit the resolution of the images being pro-

duced. Recent technical advances have increased the ease of use, and others have achieved an excellent resolution at a higher field strength (Yooyongwech et al. 2008).

Our previous report (Kalcsits et al. 2009) showed temperature to be a significant factor regulating dormancy induction in certain hybrid poplar clones. This provided a valuable system with which to further articulate the involvement of water in dormancy induction. Thus, two hybrid poplar clones, 'Walker', a temperature-sensitive clone and 'Okanese', a temperature-insensitive clone, were exposed to temperature treatments that were known to differentiate their dormancy responses. The  $T_1$  and diffusion-weighted images were obtained to investigate if there was a relation between the biophysical properties of water and dormancy induction in axillary buds of woody plants.

## Materials and methods

### *Plant material and growing conditions*

Hybrid poplar (*Populus* spp.) clones used in these experiments were interspecific hybrids from native and exotic species developed by Agriculture and Agri-Food Canada breeding stations at Indian Head, Saskatchewan (50°30.7' N) and Morden, Manitoba (49°11' N). 'Walker' is a cross of *P. deltoides* and *P. × petrowskyana*. 'Okanese' is a progeny from 'Walker'. Dormancy induction in 'Okanese' and 'Walker' is relatively temperature insensitive and temperature sensitive, respectively. Contrasting dormancy patterns in these clones under different temperature treatments allow us to compare the changes in water with the changes in dormancy.

Hardwood cuttings were propagated from hardwood cuttings in Spencer-Lemaire (Spencer-Lemaire Industries, Edmonton, Alberta) root trainers filled with soil-less media (Sunshine No. 4, Sun Gro Horticulture Inc., Bellevue, WA) and grown in a greenhouse (20 ± 5 °C) under natural light supplemented with 400 W high-pressure sodium lights (18 h photoperiod, 600 μmol m<sup>-2</sup> s<sup>-1</sup>). The rooting media were kept constantly moist during the rooting and establishment period (about 2 weeks). Cuttings were watered when required, usually every 1 or 2 days. Plants were fertilized with 100 ppm 20-20-20 water-soluble fertilizer + micronutrients once every week for the first 2 weeks and twice per week after 2 weeks. After 5–6 weeks of growth in the greenhouse (plants 30–45 cm tall), uniformly sized plants were selected and subjected to experimental treatments in growth chambers and grown over a period of 60 days.

Controlled environment chambers (Conviron model PGR15, Winnipeg, MB) were located at the phytotron facility in the College of Agriculture and Bioresources at the University of Saskatchewan. Well-established protocols were adapted to induce dormancy (Welling et al. 1997, Rinne et al. 1998, Granhus et al. 2009). Two day–night temperature

treatments were used during the induction period. Day temperature was 18.5 °C for both treatments, and night temperature was 3.5 or 13.5 °C. In addition to temperature, growth conditions in the chambers were as follows: light intensity was about 300  $\mu\text{mol m}^{-2} \text{s}^{-1}$  produced by an even ratio of incandescent and fluorescent lights; and humidity was about 40–60% RH. Plants were exposed to 12 h photoperiods, similar to the average photoperiod present during September in Saskatoon, Saskatchewan (52°7' N) for 30 days. After 30 days, day length was reduced to 10 h to simulate the shorter autumn daylight period, and plants were grown for another 30 days. The plants were watered when required, normally once every 1 or 2 days. They were fertilized with 100 ppm 20-20-20 water-soluble fertilizer + micronutrients twice per week for the first 3 weeks and once per week from that point to the end of the 60-day induction period. The plants were not allowed to dry at any time.

Growth cessation occurred at 28 days in Walker and Okanese under the warm night treatment, at 33 and 56 days in Okanese and Walker, respectively, under the cool night regime. Once this occurred, dormancy began to develop in the plants.

#### Sample collection and preparation

Plant samples ( $N = 3$ ) were collected at 0, 40 and 60 days during the induction treatment for NMR analysis. Axillary buds ( $N = 8$ ) randomly chosen from the three plant samples, about 15 cm from a terminal bud, were selected to ensure maturity of stem tissue. Stem sections were cut 2 cm below and above the selected axillary bud. The stem section with the axillary bud was placed in 10 cm NMR-sample tubes with moist cotton balls to prevent dehydration. Dormancy levels were also assessed, on the same plants used for NMR, at 0, 40 and 60 days, with a

bud-break assay that was previously described in Rinne et al. (1998). This assay uses forcing conditions (incise cuttings, maintained in water culture under long days and warm nights) where most buds eventually will break the dormancy. In actively growing clones, budbreak was about 5 days. Without forcing, the plants do not resume growth until a chilling treatment is applied.

#### NMR microimaging and data processing

Microimaging experiments were conducted using a Bruker AM (Bruker Biospin, Milton, Ontario) 8.45 T, wide-bore spectrometer equipped with the standard microimaging accessories located at the Plant Biotechnology Institute (PBI) in Saskatoon, SK, Canada. Data was collected in a  $128 \times 128$  array, using a 10.5 mm (i.d.) radio frequency coil. An orientation matrix was designed to orient slices to ensure uniformity across samples. Four image slices (1.0 mm thick) were produced from each of the three buds ( $N = 3$ ): two slices corresponding to the stem and vascular branching into the axillary meristem, and two slices for the axillary bud (Figure 1). Because of its small size, it was extremely difficult to consistently image the meristem without including superior and inferior volumes. Thus, the ROIs (about 100 pixels) selected were the vascular stem tissue, vascular bud trace and axillary bud regions.

Diffusion-weighted images were acquired using a spin-echo diffusion-weighted sequence with weighting factors of 30, 275 and 845  $\text{s mm}^{-2}$  (Stejskal and Tanner 1965). These weighting factors were empirically determined to provide adequate differentiation of diffusing water isochromats (populations) in this system. Higher weighting factors encode less mobile water molecules such as tissue water, whereas lower weighting factors sample the more mobile interstitial water populations. Thus, in this cultured poplar system, the

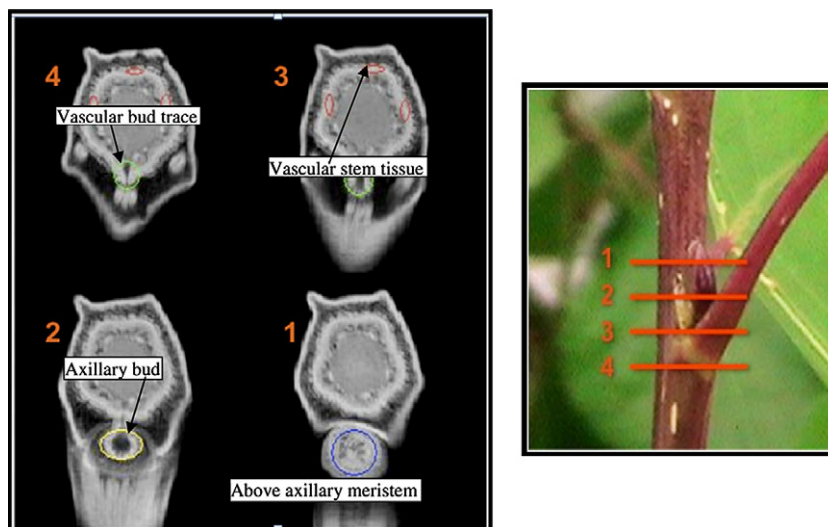


Figure 1. MRMI cross-sectional images of poplar clone, Walker, illustrating the sampling strategy. The numbered images correspond to the numbered level marks in the photograph. Within an image the regions selected for determining the  $T_1$  relaxation rates and diffusion coefficients are identified. This figure appears in color in the online version of *Tree Physiology*.

detected populations included both the extracellular water and water in vascular tissue and the intracellular or otherwise restricted water. Weighting factors ( $b$ ) were plotted against intensity ( $I$ ). The best-fit equation was extrapolated to determine  $I_0$  ( $Y$ -intercept). To calculate ADC, the two higher weighting factors (275 and 845  $\text{s mm}^{-2}$ ), presumed to preferentially sample intracellular or other less mobile fractions, were used. The ADC was calculated from

$$\text{ADC} = [\ln(I_0 - I_{b_2}) - \ln(I_0 - I_{b_1})] / (b_2 - b_1),$$

where  $b_1$  and  $b_2$  are instrument-dependent constants (275 and 845  $\text{s mm}^{-2}$ ) and  $I_{b_1}$  and  $I_{b_2}$  are the corresponding observed pixel intensities (Stejskal and Tanner 1965). Higher ADC values represent an increased water mobility within the sample tissue. Pixel ADC values were averaged over each ROI, and the data was analyzed using a two-way ANOVA ( $\alpha = 0.05$ ), where clone and temperature regime were fixed effects. Paired  $t$  tests ( $\alpha = 0.05$ ) were used to determine the differences between treatments.

The  $T_1$ -weighted images were produced using a spin-echo  $T_1$ -weighted program. Three sets of images corresponding to three TR (repetition time,  $T_1$  weighting factor) values of 100, 500 and 1000 ms were produced. Mean intensity values for each ROI ( $I$ ) were plotted against TR and  $T_1$  values calculated using the equation:

$$I = I_0(1 - e^{-\text{TR}/T_1}),$$

where  $I$  is the pixel intensity measured at TR and  $I_0$  is the maximum intensity (measured after full relaxation) (Ernst et al. 1990).

Higher  $T_1$  relaxation times correspond to a higher free water content and, conversely, to a less viscous environment. Once the  $T_1$  values were calculated for each ROI in each sample, the data was analyzed using a three-way ANOVA ( $\alpha = 0.05$ ) for each ROI where day, clone and temperature regime were fixed effects. Paired Student's  $t$  tests ( $\alpha = 0.05$ ) were used to determine the differences between ROIs.

## Results

### *Dormancy development*

Some dormancy development occurred in all induction treatments. However, the 'Days to Budbreak' metric for dormancy differed among clones and temperature treatments (Figure 2) ( $P < 0.05$ ,  $N = 8$ ,  $df = 7$ ). 'Days to Budbreak' was greater under the 18.5/13.5 °C induction treatment than under the 18.5/3.5 °C induction treatment in both 'Walker' and 'Okaneese'. Under the 18.5/13.5 °C induction treatment, there was no significant difference in dormancy development between 'Walker' and 'Okaneese' (Figure 2) ( $P < 0.05$ ,  $N = 8$ ,  $df = 7$ ). In the 18.5/3.5 °C induction treatment, 'Days to Budbreak' was significantly

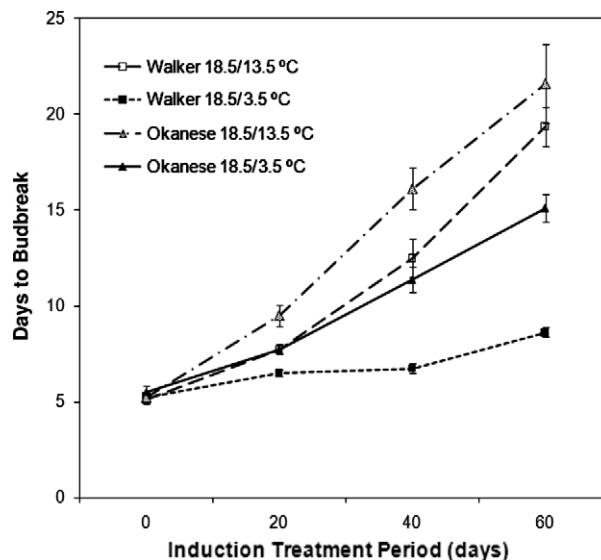


Figure 2. Dormancy development as measured by Days to Budbreak in 'Walker' and 'Okaneese' poplar clones under two temperature treatments during 60 days of short photoperiod (12 h) conditions ( $N = 8$ ). Error bars are  $\pm$  SE of the mean values.

greater in 'Okaneese' than in 'Walker' ( $P < 0.05$ ,  $N = 8$ ), indicating that dormancy development is more sensitive to night temperature in 'Walker' than in 'Okaneese'.

### *Water mobility measured by diffusion-weighted imaging*

Water diffusion-weighted images (Figure 3) were acquired to calculate the ADC for the ROI. In the diffusion-weighted images (Figure 3B and C), bright areas correspond to compartments with restricted diffusion. A visual comparison of unweighted (Figure 3A) and diffusion-weighted images (Figure 3B and C) reveals the differential tissue contrast available with incrementing weighting values. At the highest weighting value (Figure 3C), only the restricted intracellular

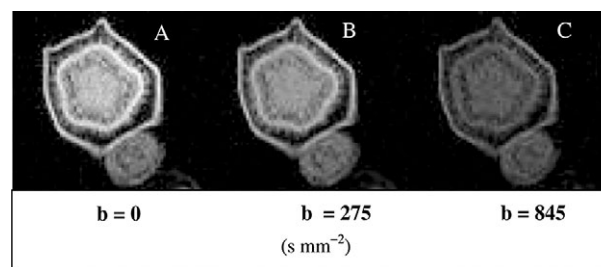


Figure 3. Diffusion-weighted images of the untreated hybrid poplar clone 'Walker'. The image series illustrates the differential tissue contrast provided by diffusion weighting. In these images, areas that contain highly mobile water become darker as the weighting factor is increased. Diffusion restricted water populations are less affected by the increasing weighting. (A) weighting factor  $b = 0$ ; (B) weighting factor  $b = 275 \text{ s mm}^{-2}$  and (C) weighting factor  $b = 845 \text{ s mm}^{-2}$ .

and interstitial water contributed significantly to the image. The ADC was calculated for ROI. The ADC was the highest in the stem vascular tissue region ( $8.77\text{--}13.98\text{ mm}^2\text{ s}^{-1}\text{ }10^{-4}$ ) and lowest in the axillary bud region ( $3.13\text{--}5.85\text{ mm}^2\text{ s}^{-1}\text{ }10^{-4}$ ). The ADC of the vascular bud trace ( $2.68\text{--}6.71\text{ mm}^2\text{ s}^{-1}\text{ }10^{-4}$ ) was intermediate to the ADC values for the stem vascular tissue and axillary bud tissues

The temperature treatments appeared to change the biophysical properties of the tissue water. In Figure 4, sample images from the temperature treatment series illustrate the differential effect of temperature on compartment water diffusion. For example, water in the central pith region of Walker demonstrated little variation in diffusivity under the low night temperature regime (Figure 4, row 1). Where the growth regime induced substantial dormancy, significant changes were observed (Figure 4, rows 2–4). For example, attenuation of the water signal from the pith region was notable. Generally, ADC decreased in all tissues in all clones during treatment. Over the 60-day induction period, the ADC decreased in the vascular stem tissue region by 32% and 1% for ‘Walker’ and by 36% and 25% for ‘Okanesse’, for the 18.5/13.5 °C and 18.5/3.5 °C

induction treatments, respectively (Figure 5). In ‘Okanesse’ at 60 days of induction, the ADC in the vascular stem tissue region was  $10.3 \times 10^{-4}$  and  $8.8 \times 10^{-4}\text{ mm}^2\text{ s}^{-1}$  for the 18.5/13.5 °C and 18.5/3.5 °C induction treatments, respectively, and was not significantly different ( $P < 0.05$ ,  $N = 3$ ,  $df = 2$ ) (Figure 5). In contrast, the ADC for ‘Walker’ at 60 days of induction from the 18.5/3.5 °C treatment was significantly greater than that from the 18.5/13.5 °C induction treatment ( $P < 0.05$ ,  $N = 3$ ,  $df = 2$ ) at  $13.9 \times 10^{-4}$  and  $9.5 \times 10^{-4}\text{ mm}^2\text{ s}^{-1}$ , respectively.

In the vascular bud trace, the ADC decreased by 56% and 3% for ‘Walker’ and by 60% and 54% for ‘Okanesse’ under the 18.5/13.5 °C and 18.5/3.5 °C induction treatments. The ADC values for ‘Walker’ were  $4.2 \times 10^{-4}$  and  $9.3 \times 10^{-4}\text{ mm}^2\text{ s}^{-1}$  and those for ‘Okanesse’ were  $3.4 \times 10^{-4}$  and  $3.8 \times 10^{-4}\text{ mm}^2\text{ s}^{-1}$ , respectively, at 60 days of induction. Relative decreases in ADC were greater in the vascular transition region than in the vascular stem tissue region. Temperature significantly influenced ADC values in the vascular stem tissue region and in the vascular bud trace region during the induction period in ‘Walker’ but not in ‘Okanesse’.

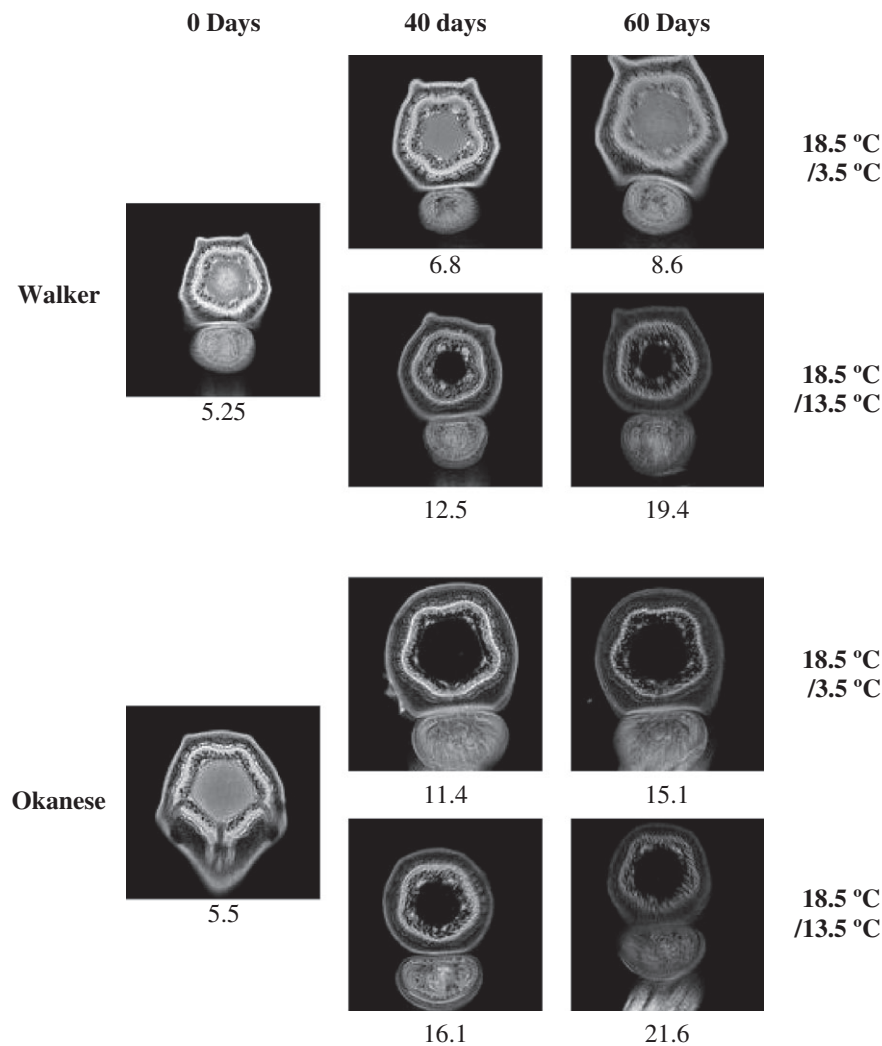


Figure 4. Cross-sectional NMR images (Level 1 from Figure 1,  $b = 0$ ) of ‘Walker’ and ‘Okanesse’ hybrid poplar (*Populus* sp.) stem and axillary bud after 0, 40 and 60 days in controlled environment chambers at 18.5/3.5 °C and 18.5/13.5 °C day/night temperature and 12 h day/night (short) photoperiod. The numbers under the images represent the mean Days to Budbreak. Visible in the images are sequential changes during the observation period as water redistributes in the observed regions. Note that the pith of those clones achieving substantial dormancy shows progressive darkening. The Day 0 Okanesse example is taken at Level 3 (Figure 1).

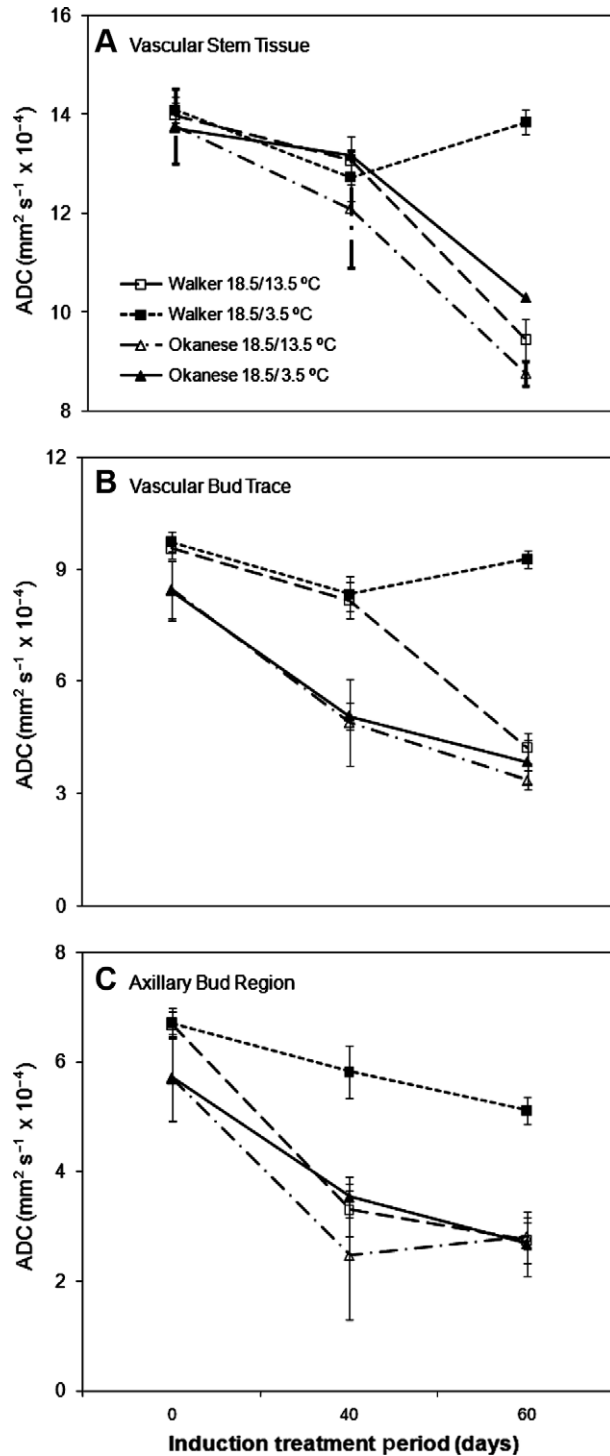


Figure 5. ADC of stem vascular tissue, vascular bud trace and axillary bud regions in ‘Walker’ and ‘Okane’ poplar clones under two induction treatments in controlled environment conditions ( $N = 3$ ). These values were calculated from diffusion-weighted series such as those shown in Figure 3. Error bars are  $\pm$  SE of the mean values.

The ADC values in the axillary bud region decreased by 59% and 23% for ‘Walker’ and by 51% and 53% for ‘Okane’, under the 18.5/13.5 °C and 18.5/3.5 °C induction

treatments, respectively. At 60 days of induction, ADC values for ‘Walker’ were  $2.8 \times 10^{-4}$  and  $5.1 \times 10^{-4} \text{ mm}^2 \text{ s}^{-1}$  and those for ‘Okane’ were  $2.8 \times 10^{-4}$  and  $2.7 \times 10^{-4} \text{ mm}^2 \text{ s}^{-1}$ , respectively.

The adaptive response to the growth treatments was apparent first in the axillary bud and vascular bud trace tissues. The stem vascular tissue exhibited no significant difference in ADC between treatments until 60 days of induction (Figure 5).

There was no decrease in ADC over time for ‘Walker’ in the 18.5/3.5 °C induction treatment. Differences in ADC were seen for clones at 40 days of induction in the vascular bud trace region but not for temperature treatment ( $P < 0.05$ ,  $N = 3$ ,  $df = 2$ ). At 60 days of induction, there was a clone–temperature interaction where ADC values decreased more under the 18.5/13.5 °C induction treatment than under the 18.5/3.5 °C treatment for ‘Walker’ but not for ‘Okane’. There were also clone–temperature interactions apparent at 60 days for the ADC values in the axillary bud region, but these were already observed at 40 days of induction. The ADC decreased more in the 18.5/13.5 °C induction treatment than in the 18.5/3.5 °C treatment for ‘Walker’ ( $P < 0.05$ ,  $N = 3$ ,  $df = 2$ ). However in ‘Okane’, the decrease in ADC over time was the same under both induction treatments.

#### $T_1$ -weighted experiments

Relaxation times are commonly measured to reflect viscosity in the ROI. Higher  $T_1$  relaxation times suggest an increased water activity, a decreased binding or a combination of both. In general, mean  $T_1$  relaxation times were highest in the vascular stem tissue region (452–1030 ms), intermediate in the vascular bud trace region (ranging from 219 to 564 ms) and lowest within the axillary bud region (ranging from 177 to 356 ms) (Figure 6). There was a significant decrease in  $T_1$  times for ‘Walker’ in all tissues at 40 days of induction ( $P < 0.05$ ,  $N = 3$ ,  $df = 2$ ) for both temperature treatments, but there was no further decrease at 60 days. The  $T_1$  relaxation times for ‘Okane’ did not change over time in the axillary bud or vascular bud trace region, but did show a small decrease in the stem vascular tissue region ( $P < 0.05$ ,  $N = 3$ ,  $df = 2$ ). The stem vascular tissue region exhibited a tendency of lower  $T_1$  times at 40 and 60 days of induction. Unlike ADC, temperature treatments did not produce wide differences in  $T_1$  relaxation times for either poplar clone (Figure 6). Although the vascular bud trace region did reveal a transient lower  $T_1$  relaxation time for the 18.5/13.5 °C temperature treatment in ‘Walker’ at 40 days, this difference disappeared by 60 days. The change in  $T_1$  relaxation times during the induction period was more linear for ‘Walker’ in the 18.5/3.5 °C than in the other induction treatment and for ‘Okane’ in both induction treatments. Initially,  $T_1$  values of ‘Walker’ were higher than those of ‘Okane’ in all regions that were examined (Figure 6).

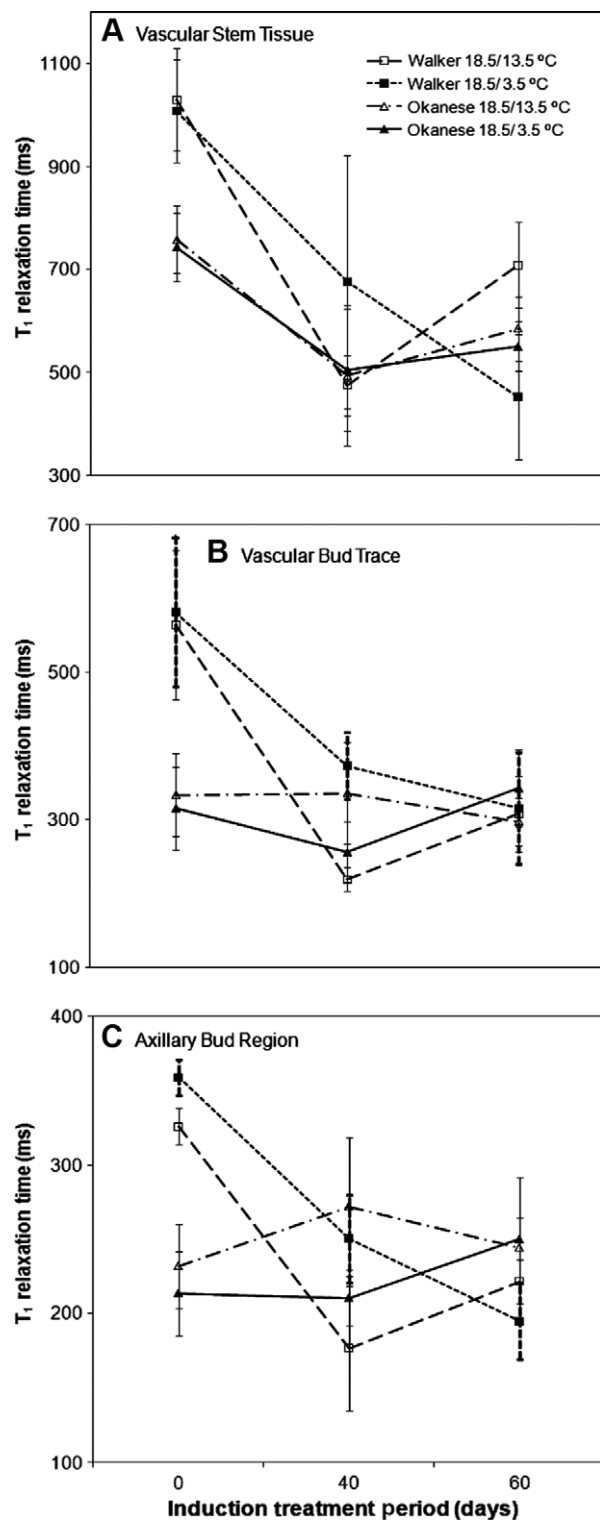


Figure 6. The  $T_1$  relaxation times of stem vascular tissue, vascular bud trace and axillary bud regions in 'Walker' and 'Okanese' poplar clones determined under two induction treatments in controlled environment conditions ( $N = 3$ ). These values were calculated from a series of images where the time between successive acquisitions is incremented to allow calculation of the longitudinal relaxation coefficient  $T_1$ . Error bars are  $\pm$  SE of the mean values.

Table 1. Correlation coefficients for ADC and  $T_1$  relaxation times and dormancy development in hybrid poplar ( $N = 9$ ,  $df = 7$ ).

| ROI                  | ADC<br>( $r$ value) | $T_1$ relaxation time<br>( $r$ value) |
|----------------------|---------------------|---------------------------------------|
| Stem vascular tissue | -0.79*              | -0.65*                                |
| Vascular bud trace   | -0.90*              | -0.36                                 |
| Axillary bud         | -0.92*              | -0.25                                 |

\*Values significantly different at the 0.05 level.

#### Correlation between dormancy development and ADC and $T_1$ relaxation times

Overall, ADC was more highly correlated with bud dormancy development than  $T_1$  relaxation times (Table 1) within the measured tissues. The ADC values for the stem vascular tissue, vascular bud trace and axillary bud regions showed a significant negative correlation with dormancy in axillary buds during the induction period. Correlations of dormancy to ADC were greatest for the vascular bud trace region ( $-0.90$ ,  $P < 0.05$ ,  $N = 9$ ,  $df = 7$ ) and the basal axillary bud ( $-0.92$ ,  $P < 0.05$ ,  $N = 9$ ,  $df = 7$ ). There was a significant negative correlation between  $T_1$  times in the stem vascular tissue and dormancy development ( $P < 0.05$ ,  $N = 9$ ,  $df = 7$ ). However,  $T_1$  relaxation times did not reflect the observed dormancy induction patterns at 40 and 60 days under warm night temperatures, and thus, this correlation appears to be weak. Changes in  $T_1$  times in the other regions did not significantly correlate with dormancy levels that were observed during the induction period.

#### Discussion

The axillary bud and vascular bud trace regions appear to be closely involved in dormancy development. We note here that the most immediate decrease in ADC under dormancy inducing conditions occurred in the axillary bud followed by the vascular bud trace region. Fennell and Line (2001) determined that water in the *Vitis*  $\times$  spp. cortex/gap tissue, between the vascular stem tissue and the axillary bud, rapidly decreases during dormancy induction. The importance of these tissues was also noted by Yooyongwech et al. (2008), who recently reported that aquaporin expression in the basal bud region was most closely associated with changing dormancy status compared to other regions examined. Quamme (1995) reported that cells in the basal region of peach buds were smaller and contained smaller vacuoles than those in subtending tissues. Ashworth (1982) described an undeveloped vascular tissue at the base of axillary buds in peach which restricted water movement between the bud and the cambium tissue and appeared to allow supercooling in dormant buds. These observations predisposed us to anticipate a reduction in water mobility in the axillary bud and vascular bud trace regions, thereby

limiting hormonal or physiological communication between the axillary bud and the stem.

The control of dormancy in woody plants appears to be regulated within the axillary bud (Fuchigami et al. 1982, Rinne et al. 2001). Cell-to-cell communication is integral in regulating meristematic growth and may be restricted during dormancy (Rinne et al. 2001). Jian et al. (1997) showed a blockage in the plasmodesmata in concert with dormancy induction in poplar buds. Furthermore, Rinne and Van der Schoot (2003) identified the presence of 1,3- $\beta$ -D-glucan that narrows or blocks plasmodesmata, thereby controlling cell-to-cell movement of metabolites in the apical meristem. If present, this represents a restriction on water movement and would be reflected as a reduction in ADC, and this is what we observed. Support for this postulate might be obtained by examining the ADC changes during dormancy release. Chilling (dormancy release) increases 1,3- $\beta$ -glucanase activity in the plasmodesmata of dormant woody plants (Rinne et al. 2001, Rinne and Van der Schoot 2003). Degradation of the 1,3- $\beta$ -D-glucan should reduce barriers to diffusion and be reflected as a local ADC increase.

The  $T_1$  relaxation did not correspond as closely with dormancy development during the induction period as did ADC. These results differ from past studies where dormancy was linked to a decrease in  $T_1$  and  $T_2$  relaxation values (Faust et al. 1991, Liu et al. 1993). These contrasting results may be attributed, in part, to the different experimental conditions. The  $T_1$  and  $T_2$  relaxation times are parameters that reflect changes in sample water content, viscosity and binding. This study used dormancy inducing conditions rather than conditions that promote release from a previously acquired dormancy. In the latter case, any confounding effects of (for example) cold acclimation are not resolved; here, the combination of genotype and temperature regime permitted some separation of these effects. As a result, we may suggest that ADC changes, but not necessarily relaxation rate changes, are linked to dormancy induction, whereas cold acclimation produces both relaxation rate and diffusion changes. Consistent with our findings, Yooyongwech et al. (2008) recently reported that an increase in ADC could be used as a marker of ecodormancy release in peach flower buds indicating a complementary effect to that observed in this dormancy induction study.

However, it must be acknowledged that not all diffusion studies are consistent with our findings. De Fay et al. (2000) measured both the ADC and  $T_2$  relaxation times in tulip bulbs during chilling and found that the ADC did not decrease during chilling. While other factors may play a role, it is important to note that the image resolution was not high and this may have resulted in a partial-volume effect that blurred responses from critical regions.

Accumulation of hydrophilic molecules such as sugars (Palonen 1999, Cox and Stushnoff 2001, Kuroda and Sagisaka 2001) and of proteins (Rinne et al. 1998), such

as occurs during cold acclimation, increases cellular-water viscosity, contributing to a decrease in  $T_1$  relaxation coefficients. A decrease in tissue water content is observed during dormancy induction (Jeknic and Chen 1999, Wake and Fennell 2000, Welling et al. 2002, Li et al. 2003). A lower water content will increase intracellular viscosity. Gardea et al. (1994), using  $^1\text{H-NMR}$  spectroscopy, reported changes in water status in grape buds under exposure to short photoperiods. However, these changes were averaged over whole buds and were evident in synchronized derivative spectra, not in relaxation maps. In the ROI selected here, water content did not change significantly. There were other tissues, such as the pith, that indicated a decrease in water content (indicated by a progressive darkening of the center of the stem in samples as shown in Figure 3) but were not a sampled 'ROI'. Thus, while  $T_1$  times in ROI did not indicate a decrease in water content, decreases in water content in the pith may account for the discrepancies between this study and previous studies using non-tissue-specific water measurements.

In conclusion, we have shown that water mobility, indicated by reduced ADC in specific tissues, correlated with the level of dormancy achieved by cultured hybrid poplar. In addition, in these studies, the ADC parameter more closely correlated with dormancy development than did the  $T_1$  relaxation time of the same tissue. We demonstrated that the ADC measurements in the axillary bud and vascular bud trace regions correlated better with dormancy development than did the vascular tissue measurements. In addition, the axillary bud region demonstrated the greatest sensitivity to temperature-induced dormancy. These changes lend strength to theories that localized biochemical and physiological changes within vascular and meristematic tissues underlay dormancy development in woody plants. With the improvement of MRMI technology increasing image resolution, it is becoming possible to resolve and study the properties of smaller tissues. With further improvement in resolution and accuracy in sampling locations, the use of ADC as a measure of water mobility and as a reflection of dormancy development is promising for dormancy studies on woody plants.

### Funding

This study was funded in part by a grant obtained through the Agroforestry Division of Agriculture and Agri-Food Canada (Indian Head, SK).

### Acknowledgments

The authors are grateful to Sue Abrams and Brock Chatson (NRC-PBI) in Saskatoon for the use of the NMR facilities. Very helpful discussions with Anne Fennell and Yuguang Bai are also gratefully acknowledged.



## References

- Ashworth, E.N. 1982. Properties of peach buds which facilitate supercooling. *Plant Physiol.* 70:1475–1479.
- Connelly, A., J.A.B. Lohman, B.C. Loughman, H. Quiquampoix and R.G. Ratcliffe. 1987. High resolution imaging of plant tissues by NMR. *J. Exp. Bot.* 38:1713–1723.
- Cox, S.E. and C. Stushnoff. 2001. Temperature-related shifts in soluble carbohydrate content during dormancy and cold acclimation in *Populus tremuloides* L. *Can. J. For. Res.* 31:730–737.
- De Fay, E., V. Vacher and F. Humbert. 2000. Water-related phenomena in winter buds and twigs of *Picea abies* L. (Karst.) until bud-burst: a biological, histological and NMR study. *Ann. Bot.* 86:1097–1100.
- Erez, A., M. Faust and M.J. Line. 1998. Changes in water status in peach buds in induction, development and release from endodormancy. *Sci. Hortic.* 73:111–123.
- Ernst, R., G. Bodenhausen and A. Wokaun. 1990. Principles of nuclear magnetic resonance in one and two dimension. Oxford University Press, 202 p (Reprint).
- Faust, M., D. Liu, M.M. Millard and G.W. Stutte. 1991. Bound versus free water in dormant apple buds – a theory for endodormancy. *Hortscience* 26:887–890.
- Faust, M., D. Liu, M.J. Line and G.W. Stutte. 1995. Conversion of bound water to free water in endodormant buds of apple is an incremental process. *Acta Hortic.* 395:113–117.
- Fennell, A. and M.J. Line. 2001. Identifying differential tissue response in grape (*Vitis riparia*) during induction of endodormancy using nuclear magnetic resonance imaging. *J. Am. Soc. Hortic. Sci.* 126:681–688.
- Fennell, A., C. Wake and P. Molitor. 1996. Use of <sup>1</sup>H-NMR to determine grape bud water state during the photoperiodic induction of dormancy. *J. Am. Soc. Hortic. Sci.* 121:1112–1116.
- Fuchigami, L.H., C.J. Weiser, K. Kobayashi, R. Timmis and L.V. Gusta. 1982. A degree growth stage (°GS) model and cold acclimation in temperate woody plants. *In Plant Cold Hardiness and Freezing Stress*. Eds. P.H. Li and A. Sakai. Academic Press, New York.
- Gardea, A.A., L.S. Daley, R.L. Kohnert, A.H. Soeldner, L. Ning, P.B. Lombard and A.N. Azarenko. 1994. Proton NMR signals associated with eco- and endodormancy in winegrape buds. *Sci. Hortic.* 56:339–358.
- Granhuis, A., I.S. Fløistad and G. Sjøgaard. 2009. Bud burst timing in *Picea abies* seedlings as affected by temperature during dormancy induction and mild spells during chilling. *Tree Physiol.* 29:497–503.
- Hou, J.Q., E.J. Kendall and G.M. Simpson. 1997. Water uptake and distribution in non-dormant and dormant wild oat (*Avena fatua* L.) caryopsis. *J. Exp. Bot.* 48:683–692.
- Ishida, N. 2000. The NMR microscope: a unique and promising tool for plant science. *Ann. Bot.* 86:259–278.
- Jeknic, Z. and T.H.H. Chen. 1999. Changes in protein profiles of poplar tissues during the induction of bud dormancy by short-day photoperiods. *Plant Cell Physiol.* 40:25–35.
- Jian, L., P.H. Li, L. Sun and T.H.H. Chen. 1997. Alterations in ultrastructure and subcellular localization of Ca<sup>2+</sup> in poplar apical bud cells during the induction of dormancy. *J. Exp. Bot.* 48:1195–1207.
- Kalsits, L., S. Silim and K. Tanino. 2009. Warm temperature accelerates short photoperiod-induced growth cessation and dormancy induction in hybrid poplar (*Populus* × spp.). *Trees: Struct. Funct.*, doi:10.1007/s00468-009-0339-7.
- Kuroda, H. and S. Sagisaka. 2001. Ultrastructural changes in apical meristem cells of apple flower buds associated with dormancy and cold tolerance. *J. Jpn. Soc. Hortic. Sci.* 70: 553–560.
- Li, C., O. Junntila, A. Ernsteen, P. Heino and E.T. Palva. 2003. Photoperiodic control of growth, cold acclimation and dormancy development in silver birch (*Betula pendula*) ecotypes. *Physiol. Plant.* 117:206–212.
- Liu, D., M. Faust, M.M. Millard, M.J. Line and G.W. Stutte. 1993. States of water in summer-dormant apple buds determined by proton magnetic resonance imaging. *J. Am. Soc. Hortic. Sci.* 118:632–637.
- Palonen, P. 1999. Relationship of seasonal changes in carbohydrates and cold hardiness in canes and buds of three red raspberry cultivars. *J. Am. Soc. Hortic. Sci.* 124:507–513.
- Quamme, H.A. 1995. Deep supercooling in buds of woody plants. *In Biological Ice Nucleation and its Applications*. Eds. R.E. Lee, G.J. Warren and L.V. Gusta. American Phytopathological Society, St. Paul, MN, pp 183–200.
- Rinne, P.L.H. and C. Van der Schoot. 2003. Plasmodesmata at the crossroads between development, dormancy and defense. *Can. J. Bot.* 81:1182–1197.
- Rinne, P., A. Saarelainen and O. Junntila. 1994. Growth cessation and bud dormancy in relation to ABA level in seedlings and coppice shoots of *Betula pubescens* as affected by a short photoperiod, water stress and chilling. *Physiol. Plant.* 90:451–458.
- Rinne, P., A. Welling and P. Kaikuranta. 1998. Onset of freezing tolerance in birch (*Betula pubescens* Ehrh.) involves LEA proteins and osmoregulation and is impaired in an ABA-deficient genotype. *Plant Cell Environ.* 21:601–611.
- Rinne, P.L.H., P. Kaikuranta and C. Van der Schoot. 2001. The shoot apical meristem restores its symplastic organization during chilling-induced release from dormancy. *Plant J.* 26:249–264.
- Snaar, J.E.M. and H. Van As. 1992. Probing water compartments and membrane permeability in plant cells by <sup>1</sup>H NMR relaxation measurements. *Biophys. J.* 63:1654–1658.
- Stejskal, E.O. and J.E. Tanner. 1965. Spin diffusion measurements: spin echoes in the presence of a time-dependent field gradient. *J. Chem. Phys.* 42:288–292.
- Tanner, J.E. 1983. Intracellular diffusion of water. *Arch. Biochem. Biophys.* 224:416–428.
- Van der Toorn, A., H. Zemah, H. Van As, P. Bendel and R. Kamensky. 2000. Regulation of growth, development and whole organism physiology: developmental changes and water status in tulip bulbs during storage: visualization by NMR imaging. *J. Exp. Bot.* 51:1277–1287.
- Wake, C.M.F. and A. Fennell. 2000. Morphological, physiological and dormancy responses of three *Vitis* genotypes to short photoperiod. *Physiol. Plant.* 109:203–210.
- Welling, A., P. Kaikuranta and P. Rinne. 1997. Photoperiodic induction of dormancy and freezing tolerance in *Betula pubescens*: involvement of ABA and dehydrins. *Physiol. Plant.* 100:119–125.
- Welling, A., T. Moritz, E.T. Palva and O. Junntila. 2002. Independent activation of cold acclimation by low temperature and short photoperiod in hybrid aspen. *Plant Physiol.* 129:1633–1641.
- Yooyongwech, S., A.K. Horigane, M. Yoshida, M. Yamaguchi, Y. Sekozawa, S. Sugaya and H. Gemma. 2008. Changes in aquaporin expression and magnetic resonance imaging of water status in peach tree flower buds during dormancy. *Physiol. Plant.* 134:522–533.